ACCSCIENCE PUBLISHING

Materials Science in Additive Manufacturing

ORIGINAL RESEARCH ARTICLE

Unlocking the sustainable potential of 3D concrete printing with large aggregates and steam–CO_2 curing

Suvash Chandra Paul[1]*, Junghyun Lee[1], Yi Wei Daniel Tay[1], Sean Gip Lim[1], Jihye Jhun[1], Bandar A. Fadhel[2], Issam T. Amr[2], and Ming Jen Tan[1]*

[1]Singapore Centre for 3D Printing, School of Mechanical and Aerospace Engineering, College of Engineering, Nanyang Technological University, Singapore

[2]Saudi Aramco Research & Development Center, Dhahran, Eastern Province, Saudi Arabia

Abstract

Three-dimensional concrete printing (3DCP) has emerged as a promising innovation in the construction industry, significantly reducing its reliance on intensive labor while minimizing material waste. Despite its benefits, a major limitation of current 3DCP practices is the high reliance on cement as the primary binder, which often exceeds 60% of the total solid content. This high cement usage contributes significantly to CO_2 emissions, raising sustainability concerns. In this study, a 3D-printable concrete mix incorporating large aggregates (up to 10 mm) was developed, replacing over 7% of fine aggregate and reducing cement content to approximately 29% by weight. The effects of CO_2 gas and a steam–CO_2 mixture on the mechanical performance and CO_2 uptake of the printed concrete were assessed. Thermogravimetric analysis was used to quantify CO_2 sequestration over time. Compared to control samples without gas treatment, those exposed to the steam–CO_2 mixture showed enhanced buildability, improved compressive and flexural strength, and greater CO_2 uptake. The results suggest that surface spraying of the steam–CO_2 mixture during the 3D printing process offers a viable and scalable approach to improving both the structural performance and environmental footprint of printed concrete elements.

Keywords: 3D concrete printing; Carbon dioxide uptake; Large-aggregate printing; Steam–CO_2 injection; 3DCP buildability; CO_2 emission cost; Mechanical strength

***Corresponding authors:**
Suvash Chandra Paul
(suvash.cp@ntu.edu.sg)
Ming Jen Tan
(mmjtan@ntu.edu.sg)

Citation: Paul SC, Lee J, Daniel Tay YW, *et al.* Unlocking the sustainable potential of 3D concrete printing with large aggregates and steam–CO_2 curing. *Mater Sci Add Manuf.* 2026;5(1):025330076. doi: 10.36922/MSAM025330076

Received: August 15, 2025

Revised: September 8, 2025

Accepted: September 12, 2025

Published Online: October 29, 2025

1. Introduction

Additive manufacturing, commonly known as three-dimensional concrete printing (3DCP) in the construction sector, offers numerous advantages,[1] including design freedom, reduced material waste, lowered labor requirements, and formwork elimination, ultimately leading to a significant reduction in costs. Once the printer is configured and the appropriate material is selected, it can print continuously without intensive human intervention until the desired structural shape is complete. Many countries have already successfully constructed functional concrete structures[2] and restored naturally formed structures[3] using three-dimensional (3D) printing technology, demonstrating its practical capabilities.

In recent years, researchers from both academia and industry have conducted extensive studies on the application of 3DCP. These efforts have primarily focused on evaluating a wide range of materials and their properties to determine their suitability for 3DCP technology.[4-6] However, unlike conventional concrete casting, 3DCP builds structures layer by layer, which can introduce anisotropic behavior and weak interlayer bonding due to pore formation.[7] The absence of compaction or vibration during printing further increases porosity, potentially reducing mechanical strength and durability.[8] These structural challenges highlight the need for enhanced material formulations and curing methods, such as the steam–CO_2 integration proposed in this study.

One major drawback of the 3DCP technology is its high binder demand. For example, the use of fine aggregate particles, typically less than 4 mm in size, requires a substantial amount of binder or cement to produce printable materials. This is because the materials need to be mixed and transported through pumps and hose pipes to the printing head or nozzle before being deposited in layers. Cement is the most used binder in both conventional and 3DCP construction processes. However, the production of cement is known to be one of the major contributors to CO_2 emissions, which contribute to atmospheric greenhouse gases. A large amount of CO_2 is released during cement manufacturing, both due to energy use and the calcination chemical process.[9] To mitigate this issue, one potential strategy is to substitute fine particles with larger aggregates in the printable materials, which would significantly decrease the amount of cement used and associated carbon emissions. From a sustainability perspective, alternative binder materials, such as slag, silica fume, and fly ash, can be used to replace cement. Another challenge with 3DCP is the absence of formwork, leaving most printed surfaces directly exposed to the environment. This exposure may impact the curing process and, subsequently, the mechanical and durability properties of 3DCP structures.[10,11]

Carbonation technology offers several benefits for concrete. It not only improves the properties of concrete but also permanently sequesters CO_2 in it.[12] One commonly used method of carbonation technology is curing concrete samples in a CO_2 chamber. This allows CO_2 to react with different hydration products of cement at different stages, resulting in the formation of minerals for carbon sequestration. The key reactions that take place between CO_2 and the cement matrix are illustrated in Equations I–IV.[13-15]

$$3CaO.SiO_2 + 3CO_2 + xH_2O \rightarrow SiO_2.xH_2O + 3CaCO_3 \quad (I)$$

$$2CaO.SiO_2 + 2CO_2 + xH_2O \rightarrow SiO_2.xH_2O + 2CaCO_3 \quad (II)$$

$$Ca(OH)_2 + CO_2 \rightarrow CaCO_3 + H_2O \quad (III)$$

$$C-S-H + 2CO_2 \rightarrow SiO_2 + 2CaCO_3 + H_2O \quad (IV)$$

During the carbonation reaction in cement, the primary products are calcium carbonate ($CaCO_3$) and silica (SiO_2). These products are primarily formed through the decalcification of silicate phases or dehydrated cement particles, as well as through the formation of calcium–silicate–hydrate (C–S–H) gel. In the curing process, the carbonation of tricalcium silicate ($3CaO.SiO_2$ or C_3S) and dicalcium silicate ($2CaO.SiO_2$ or C_2S) phases governs the process, resulting in the production of silica gel and calcite, as shown in Equations I and II.[13] In the weathering carbonation process, calcium hydroxide ($Ca(OH)_2$) is consumed, and $CaCO_3$ is produced, as shown in Equation III.[14] However, with excessive exposure to CO_2, the C–S–H gel decomposes, as shown in Equation IV.[15]

The presence of CO_2 in concrete lowers the pH value in the pore solution of the carbonated area. In general, natural carbonation is considered a long-term process and can result in depassivation and corrosion of the reinforcement. In addition, the rate of CO_2-related reaction in concrete depends on various factors, such as the water–cement ratio (w/c) of the concrete, the composition of materials, the type of curing, the quantity of pores, temperature, and internal humidity.[14]

In numerous studies, scientists have attempted to utilize CO_2 to directly or indirectly modify the properties of materials, both in their fresh and hardened states. The X-ray diffraction test reveals that as the concentration of CO_2 increases, the amount of calcite also increases. Conversely, in the case of portlandite, the amount decreases as CO_2 levels rise.[14] It is reported that the prolonged mixing of CO_2 can significantly impact the workability of materials. According to a report, as the duration of CO_2 exposure increases, the workability of the materials decreases.[12] This is due to the rapid hydration of C_3S and C_3A, forming $CaCO_3$ through the reaction of CO_2 with $Ca(OH)_2$. Similarly, Monkman *et al.*[16] confirmed this decreased workability behavior of materials exposed to CO_2. The initial slump value was reduced by 25–33% compared to the reference materials. Rapid hydration is also a contributing factor to the lower setting time of the materials.[12]

Researchers have investigated the effects of large aggregates on various properties of 3DCP.[17-19] The inclusion of large aggregates increases the paste volume and the thickness of the water film in mixers, reducing the yield stress and viscosity of fresh materials, ultimately

affecting printability.[17] Similar findings of decreased yield stress and viscosity have been reported by Wang *et al.*[19] Moreover, the researcher has investigated various chemical admixtures to optimize the rheological properties, such as yield stress and viscosity, of 3D-printable cementitious materials.[20]

The buildability of 3D-printable materials is reported to improve with the inclusion of large aggregates.[17] Furthermore, large aggregates can diminish the anisotropic behavior of 3D-printed samples and enhance mechanical properties, including compressive strength, flexural strength, bond strength, and elastic modulus. The redistribution of aggregates during the printing process and their penetration through the interlayer have been shown to increase bond strength and other mechanical properties in samples containing large aggregates. This redistribution positively affects the anisotropic behavior of 3D-printed samples.[18]

However, if materials are not properly selected, specifically regarding the types and content of aggregates, the inclusion of large aggregates may negatively affect the properties of 3D-printed samples.[19] Overall, positive outcomes have been reported for the use of large aggregates in 3DCP.[21,22] In addition, incorporating large aggregates can reduce the need for an excessive amount of cement and natural sand compared to conventional 3D-printed mortar mixes, potentially offering a beneficial environmental impact.[21] The use of large aggregates in printing can decrease cement volume fraction by approximately 50% compared to 3D-printed mortar mixes.[23]

This study analyzed the effects of directly injecting CO_2 and a steam–CO_2 mixture into fresh 3D-printed concrete samples incorporating large aggregates on their mechanical properties and printability. The printability of the 3D-printed materials was evaluated by assessing the maximum buildable layers of the fresh material under varying CO_2 and steam–CO_2 pressures. In addition, the hardened 3D-printed samples underwent compression and flexural testing to determine the influences of CO_2 and steam–CO_2 integration. To quantify the amount of CO_2 sequestered by the materials, a thermogravimetric analysis (TGA) test was performed. The results demonstrated that the injection of CO_2 and steam–CO_2 enhanced both the printability and mechanical strength of the large-aggregate-based 3D–printed materials compared to the control mix. To the best of the authors' knowledge, the research methodology employed in this study, involving CO_2 and steam–CO_2 injection into the large aggregates of 3D-printed concrete samples, is unique and has not been extensively documented in the scientific literature.

2. Materials and methods

2.1. Materials

Material composition is a crucial part of 3D printing technology. As a 3D-printed material undergoes mixing, pumping, and extrusion through a designated nozzle orifice, each component of the material plays a significant role in the printing process. In this study, a 3D-printable material was developed, consisting of large aggregates with a maximum size of 10 mm. These aggregates were used to replace a portion of the sand, which typically provides volumetric stability in 3DCP structures. The main materials used in this research work included ordinary Portland cement (CEM-I), undensified silica fume, a polycarboxylate superplasticizer, potable water, natural river sand (maximum size 2.3 mm), and gravel as large aggregates (maximum size of 10 mm), as presented in Table 1. The chemical compositions of the cement and silica fume utilized in this study are detailed in Table 2.

2.2. Printer and material delivery system

A six-axis robotic arm (KR 120 R3900 ultra K, KUKA, Germany) mounted with a customized nozzle (Figure 1A) was used to control the movement of the print head. Slicer software (Mastercam 2017, United States [US]) was used to create the 3D design in an XYZ coordinate system. A progressive cavity feed pump (Taurus pump, MAI

Table 1. Material compositions by weight (%) for 3D concrete printing

Materials	Weight (%)
Cement	29.3
Silica fume	2.89
Sand	48.21
Large aggregate	7.28
Water	12.02
Superplasticizer	0.29

Table 2. Chemical compositions (% w/w) of cement and silica fume used in the research

Compositions	Cement (%)	Silica fume (%)
CaO	61.09	0.68
SiO_2	18.69	95.78
Al_2O_3	6	0.12
Fe_2O_3	2.86	0.03
SO_3	2.75	-
MgO	2.55	0.42
K_2O	0.51	1.44
$Na_2O_{eq.}$	0.38	0.43

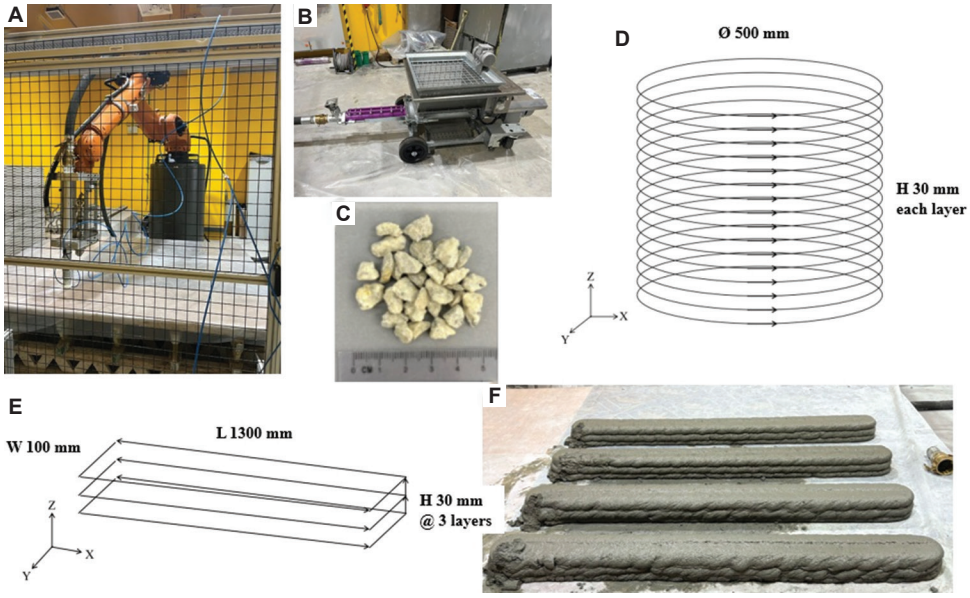

Figure 1. Set up of the 3D-printed large-aggregate concrete. (A) Six-axis robotic arm printer. (B) Pump for material delivery. (C) Large aggregates. (D) Tool path for buildability. (E) Tool path for mechanical testing samples. (F) Printed samples for mechanical properties testing

International GmbH, Austria) with a material extrusion rate of approximately 30 L/min was used as the printer's pumping system. The printer is capable of producing objects with a diameter of up to 2.5 m. It was equipped with a circular nozzle measuring 45 mm in diameter and a 50 mm-diameter hose for transporting materials to the nozzle head. The nozzle head operated at a print speed of 150 mm/s to ensure smooth printing of 3D samples for buildability and mechanical testing. Figure 1A-F illustrates the printer, pump, large aggregates, toolpaths for buildability tests, toolpaths for mechanical testing samples, and printed samples used for mechanical strength evaluation.

2.3. Steam and CO_2 injection in 3D-concrete-printing structures

Current carbon capture and sequestration methods often face challenges, including slow kinetics, limited CO_2 uptake, high costs, and lengthy processing times. In general, natural carbonation requires long-term treatment due to its slow reaction rate, which significantly increases production costs.[24] To address these issues, researchers have developed a straightforward technique that utilizes porous structures for rapid CO_2 capture.[25] However, this approach compromises the strength of concrete, as increased porosity reduces its structural integrity. Therefore, to evaluate the CO_2 sequestration efficiency, this study employed a method[26] in which pure CO_2 (99% purity) was sprayed onto the surface of the printing layer during the 3D printing of structures. CO_2 was applied at pressures of 2 bar, 4 bar, or 6 bar. In addition, to further enhance CO_2 capturing, the study also conducted experiments that involved injecting steam alongside CO_2. The effects of CO_2 spraying and steam–CO_2 spraying on the properties of 3D-printed concrete materials were compared with a control mix that did not involve CO_2 or steam injection.[24,25]

2.4. Buildability test of 3D-printed concrete

The maximum height achievable with 3DCP was determined through the material's strength, which must withstand the increasing compressive stresses from its own weight during printing. If these stresses exceed the yield strength, structural failure occurs. To assess buildability, a circular object with a 500-mm diameter was printed layer by layer vertically until it collapsed. The nozzle size and printing speed, as mentioned earlier, remained consistent throughout the experiments. The buildability of the materials was evaluated under different CO_2 pressures, both with and without steam, and their performance was compared to the control mix.

2.5. Mechanical properties and microstructure test

The samples for the compressive and flexural strength tests were obtained from the printed specimens, as shown in Figure 1F. For each testing batch conducted on different days, a minimum of four samples were collected: cubes measuring approximately 90 mm × 90 mm × 90 mm for the compression test, and prisms measuring 90 mm × 90 mm × 300 mm for the flexural test. The printing took place in a laboratory environment with an average temperature of 22 ± 2°C and relative humidity of 60 ± 5%. All samples were stored in the laboratory until

testing, and no additional curing methods were employed. It is important to note that only a CO_2 pressure of 2 bar was used for mechanical testing and CO_2 uptake calculations. Higher CO_2 pressures result in rough surfaces on the 3D-printed structures, potentially leading to uneven load distribution during mechanical testing.[27]

For the compressive strength test, a universal compression testing machine (B-001, ALFA Testing Equipment, Turkey) with a capacity of 2,000 kN was used to apply load gradually and uniformly to the samples. The loading rate was maintained at 900 N/s, in accordance with the ASTM C109/C109M standard[28] for measuring the compressive strength of hydraulic cement mortar samples. The flexural strength was determined using an Instron machine (5969, US), following the ASTM C293 standard,[29] which outlines the standard test method for flexural strength of concrete. In this test, a three-point bending load was applied to the samples, centered between two lower supports, with the distance between the supports set to three times the sample depth (i.e., 270 mm).

For microstructural analysis, images were obtained from hardened samples using a JSM 5600 LV scanning electron microscope (SEM; JEOL, Japan) with a magnification of ×100 and a scale bar of 100 μm. Small samples, measuring 2–3 mm in thickness and approximately 20 mm × 20 mm in area, were cut from the hardened concrete at 28 days of age and immersed in ethanol for an additional 7 days to halt the hydration process. Subsequently, the samples were placed in an oven at 60°C for 24 h before the SEM test. In addition, a metal coating was applied to the samples to ensure a smooth surface for testing.

2.6. Thermogravimetric analysis for the CO_2 uptake test

Thermogravimetric analysis was employed to measure mass loss resulting from the decomposition of hydration products, including ettringite, calcium silicate hydrate, calcium hydroxide, and carbonated calcium hydroxide, under different printing conditions. This mass loss reflects the decomposition of chemically bound water in the hydration products, providing an estimate of the degree of cement hydration as well as the decomposition of $CaCO_3$ corresponding to the release of CO_2 that was taken up during carbonation. For the TGA test, the peripheral region of samples from the compressive strength tests was collected after 7 and 28 days of testing. These samples were immersed in an ethanol solution for 7 days to halt the hydration process of the binders. After immersion, the samples were removed from the ethanol and placed in an oven at 60°C for 24 h. They were then ground into powder samples using a mortar and pestle and sieved through a 250-μm sieve. The prepared samples were analyzed at a ramping rate of 20°C/min over a temperature range of 25°C to 1,000°C to measure and monitor the mass loss of the concrete samples. The extent of hydration reactions and the amount of CO_2 uptake by the materials were determined using Equations V–XIII:[30]

$$Dehydration\ (Ldh) = m_{105^oC} - m_{400^oC} \quad \text{(V)}$$

$$Dehydroxylation\ (Ldx) = m_{400^oC} - m_{500^oC} \quad \text{(VI)}$$

$$Decarbonation\ (Ldc) = m_{500^oC} - m_{950^oC} \quad \text{(VII)}$$

$$Bound\ water\ (W_c) = \left(Ldh + Ldx\right) + 0.41\left(Ldc\right) \quad \text{(VIII)}$$

$$Free\ Ca\left(OH\right)_2\ (CH_f) = 4.11\left(Ldx\right) + 1.68\left(Ldc\right) \quad \text{(IX)}$$

$$Poorly\ crystalline\ CaCO_3\ (DC) = m_{500^oC} - m_{700^oC} \quad \text{(X)}$$

$$Well\ crystalline\ CaCO_3\ (HC) = m_{700^oC} - m_{950^oC} \quad \text{(XI)}$$

$$Degree\ of\ hydration\ (DOH) = 100 \times \frac{W_c}{0.24} \quad \text{(XII)}$$

$$\text{Carbon uptake}\left(\text{wt \% binder}; \xi\right) = \frac{m_{500^oC} - m_{950^oC}}{n \times (m_{105^oC} - W_c - CH_f)} \quad \text{(XIII)}$$

where n is the solid binder constitutions (wt.% dry mix), W_c is the chemically bound water (wt.% sample), and CH_f is the free calcium hydroxide (wt.% sample).

Note that the carbonation of metal oxides was not included due to its low concentration and hence was considered negligible. In addition, various methods are available for quantifying CO_2 in cement-based materials, depending on the specific materials and their decomposition processes. These methods include back-titration, Fourier-transform infrared spectroscopy, and Raman spectroscopy.[31] However, this study was limited to TGA analysis only.

3. Results and discussion

Most studies on carbonation have primarily concentrated on the carbonation curing of concrete samples or the mixing of CO_2 with aggregates or binders before combining them with other concrete constituents.[32,33] This study employed spraying techniques to apply CO_2 and steam onto the surface of freshly printed layers.

3.1. Number of buildable layers of 3D-concrete-printing structures

The number of buildable layers of the 3DCP structures under various conditions, including the presence and

absence of CO_2 and steam, is illustrated in Figures 2 and 3. It is evident that the buildability of the materials improved with increasing CO_2 pressure during printing, compared to the control mix. The maximum buildability was observed at a CO_2 spraying pressure of 6 bar. In addition, the application of steam combined with a CO_2 spraying pressure of 4 bar also showed a positive effect. Thus, it can be concluded that spraying CO_2 and steam onto the surface of the printed layers enhanced the buildability of concrete. This effect is attributed to CO_2 spraying, which aids in drying the layer's surface and reduces setting time by altering the kinetics of cement hydration. The reaction between CO_2 and CaO or $Ca(OH)_2$, after mixing with water, will produce $CaCO_3$, contributing to an increased buildable height of the 3D-printed structure. When steam is introduced alongside CO_2, the printed layer's surface becomes wet, enhancing the formation of C–S–H and $CaCO_3$ and forming a strong bond with subsequent layers, thereby enhancing the buildable layers (Figure 3A).

The material developed in this research was also used to print 1.5 m-tall walls (roughly 50 layers), as displayed in Figure 3. Figure 3B illustrates the toolpath used for wall printing, while Figure 3C displays the printed wall.

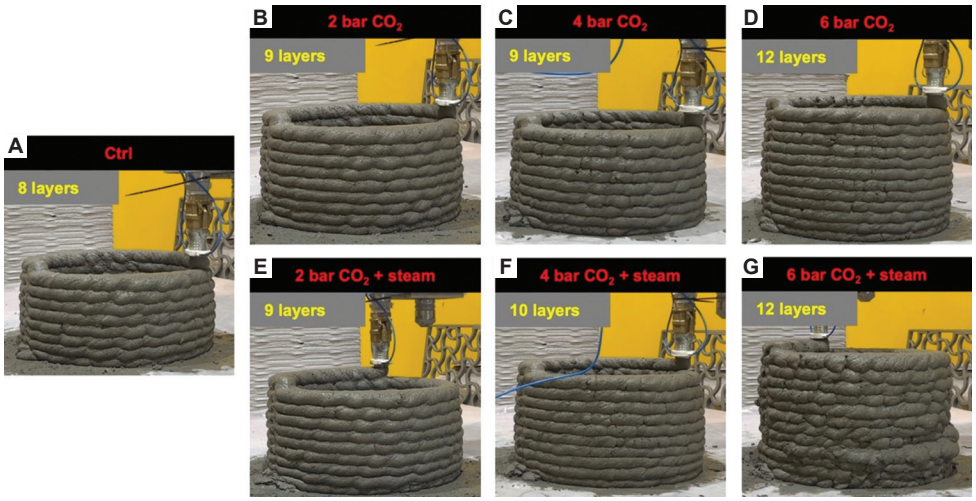

Figure 2. Buildable layers of the 3D-printed large-aggregate concrete. (A) Control mix (Ctrl). (B) CO_2 pressure of 2 bar. (C) CO_2 pressure of 2 bar with steam. (D) CO_2 pressure of 4 bar. (E) CO_2 pressure of 4 bar with steam. (F) CO_2 pressure of 6 bar. (G) CO_2 pressure of 6 bar with steam.

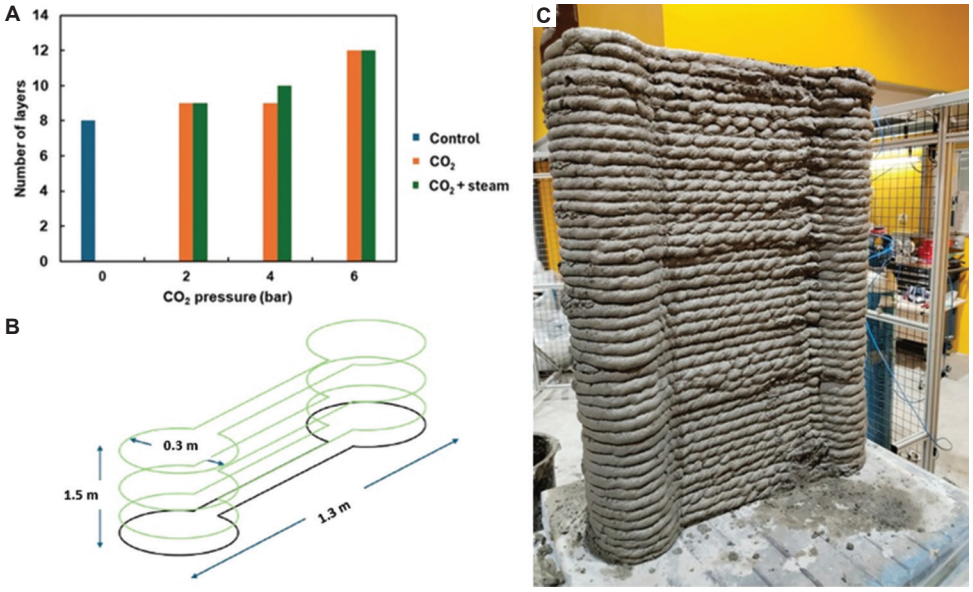

Figure 3. Buildability of large aggregate 3D printing materials. (A) Number of buildable layers across varying CO_2 pressures. (B) Toolpath and dimension for wall printing. (C) 1.5 m-high wall printed with large-aggregate concrete at a CO_2 pressure of 2 bar with steam.

During wall printing, the process was paused every 5–6 layers for 7–10 min to mix a new batch of materials. As a result, the total time to complete the wall was 90–100 min. This experiment aimed to print a scalable structure using the large-aggregate 3D-printable material, combined with a steam–CO_2 mixture as a potential alternative to traditional accelerating agents in concrete construction. This method could also serve as a means for permanent CO_2 sequestration in fresh concrete. In a previous study, Li *et al.*[12] examined the effects of directly incorporating CO_2 into materials during mixing. The study found that this approach resulted in lower workability and reduced setting time. Their SEM images further indicated that the formation of reaction products on the surface of cement grains due to CO_2 mixing accelerated the hydration of both tri-calcium aluminate (C_3A) and tricalcium sulfate (C_3S).

3.2. Compressive and flexural strength of the 3D-concrete-printing structure

The development of compressive strength and the failure patterns of 3D-printed large-aggregate samples at 7 and 28 days are illustrated in Figure 4A and B. On both days, samples treated with a steam–CO_2 mixture exhibited enhanced strength. By 28 days, the strength of the CO_2-treated and steam–CO_2-treated samples was approximately 25% and 28% higher, respectively, compared to the control sample. This improvement aligns with the buildability results. The enhanced strength can be attributed to the formation of nanoscale calcite ($CaCO_3$) particles, which refined the pore structures in the hardened concrete due to the reaction between sprayed CO_2 and the CaO in the cement.[34]

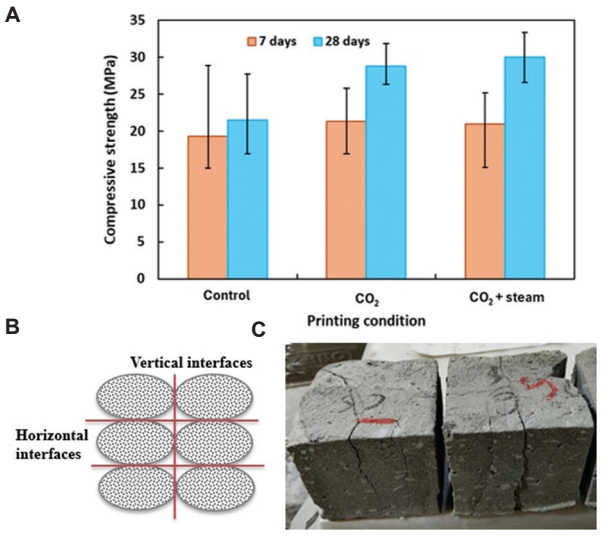

Figure 4. Strength and cracking patterns in the 3D-printed samples. (A) Compressive strength development in large-aggregate 3D-concrete-printing samples under varying conditions. (B) Illustration of a 3D-printed cube sample with a dimension of 90 mm × 90 mm. (C) Failure patterns of tested cube samples.

In 3D-printed samples, the interfaces between layers contribute to anisotropic mechanical behavior, in contrast to cast samples.[35,36] These interfaces often serve as weak points that affect the stress–strain response, energy dissipation, and crack formation.[35] Cracks can develop on both vertical and horizontal interfaces (refer to the red lines in Figure 4B), influenced by factors such as the loading orientation relative to the printed sample, the type of loading (bending or compression), and the dimensions of the samples. Figure 4C clearly shows that a crack occurred on the vertical interface of the cube samples before failure during the compression test. Although not depicted here, horizontal cracks were also observed in some samples. Detailed discussions on crack propagation in 3D-printed concrete samples, both with and without fibers, can be found in.[35,37]

The flexural strength of the 3D-printed samples was also enhanced with the incorporation of a steam–CO_2 mixture during printing, as shown in Figure 5. Compared to the control mix, the concrete samples sprayed with CO_2 or a steam–CO_2 mixture exhibited approximately 2% and 4% higher strength, respectively, at the 28-day mark. The strength development of flexural samples from 7 days to 28 days was not as significant as that observed in compressive strength samples. Previous research has shown that CO_2-cured concrete exhibited higher strength development at an early age of 3 days compared to water-cured conventional concrete.[38] However, this difference became negligible at later ages of 28 and 90 days for both CO_2-cured and conventional concrete samples. The size of the samples also affects the strength of CO_2-cured samples. Specifically, smaller 5 cm × 10 cm cylinder samples demonstrated greater strength development than larger sizes, such as 10 cm × 20 cm and 15 cm × 30 cm cylinders.

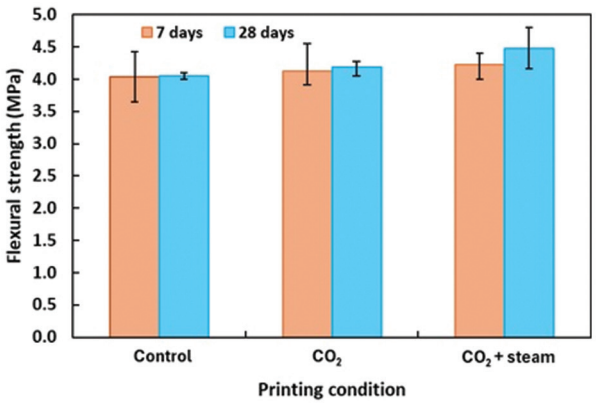

Figure 5. Flexural strength development in large-aggregate 3D-concrete-printing samples

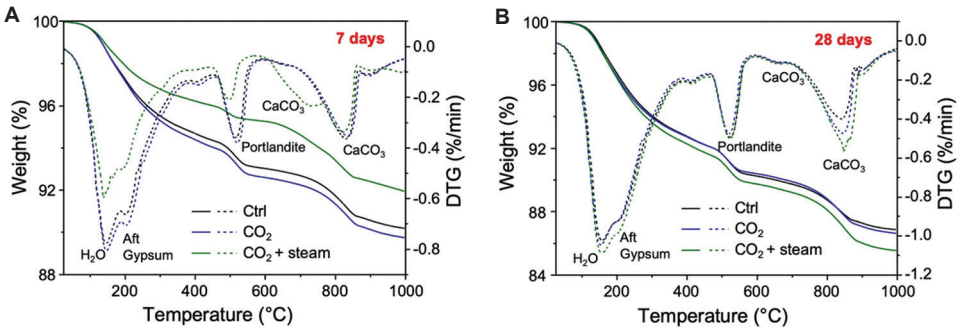

Figure 6. Thermogravimetric (TGA) and derivative thermogravimetric (DTG) curves of the 3D-printed concrete with large aggregate at (A) 7 days and (B) 28 days

In addition to sample size, curing conditions, including CO_2 pressure, concentration, and curing time, are also crucial for strength development.

Both concrete strength and the degree of CO_2 curing increase with longer curing times and higher CO_2 pressures.[39] Notably, the reaction between CO_2 and cement within the concrete occurs rapidly, within 15 min, regardless of CO_2 pressure and pre-conditioning environment. CO_2 spraying on wet concrete initiates a carbonation reaction alongside cement hydration, leading to early-age carbonation.[40] Importantly, no adverse effects on the long-term development of concrete properties have been observed due to early-age carbonation. The interaction between CO_2 and cement contributes to the formation of nanosized $CaCO_3$, which helps fill voids and improve strength. However, some researchers have reported negative effects on cement hydration caused by CO_2, attributed mainly to variations in material compositions and carbonation conditions.[41-43] Therefore, further research is needed to understand the carbon dynamics in these factors and confirm their effects on carbonated concrete.

3.3. CO_2 uptake in 3D-concrete-printing samples

As shown in Figure 6, the TGA curve and derivative thermogravimetric (DTG) curve for 3D-printed concrete samples provide invaluable information about their hydration and carbonation state. The TGA and DTG curves typically show several distinct mass loss steps, each corresponding to the thermal decomposition of different compounds present in the concrete.[25,27,44] Among them, for CO_2 sequestration of 3D-printed concrete samples, it is necessary to examine in detail the decomposition range of $CaCO_3$ located within the temperature range of 600–950°C.

At the early stage of curing (7 days), the integration of CO_2 with steam enhanced the carbonation process in the 3D-printed concrete sample, as illustrated in Figure 6A. However, the amount of CO_2 sequestration calculated using Equation XIII did not show a significant difference across

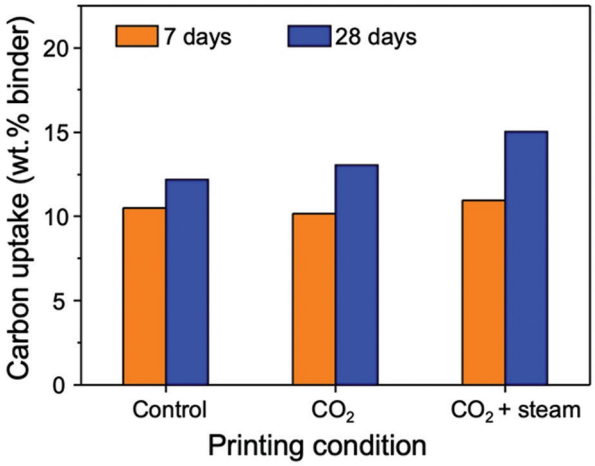

Figure 7. Comparison of CO_2 uptake under three different printing conditions at 7 and 28 days

printing conditions. At longer curing times (28 days), changes depending on printing conditions became more evident. Compared to the 7th day's TGA and DTG curves, more hydrated and carbonated products were formed. In the carbonation process, well-crystallized $CaCO_3$ can be more dominant, and the integration of CO_2 or a steam–CO_2 mixture increased the amount of well-crystallized $CaCO_3$, as shown in Figures 6B and 7. Compared to the control samples at 28 days, the CO_2 uptake of the CO_2-sprayed 3DCP samples increased by 7%, while that of the steam–CO_2-treated samples increased by 23%. The results indicate that spraying CO_2 or a steam–CO_2 mixture not only accelerates carbonation during 3D printing, thereby improving buildability but also enhances CO_2 sequestration during the curing process. These findings open new avenues for future research on varying CO_2 concentrations, pressures, and their effects on different concrete compositions for the permanent sequestration of CO_2 from the atmosphere. Moreover, CO_2 uptake in concrete depends on several factors, including the water-to-solid ratio and reaction time. Studies have shown that

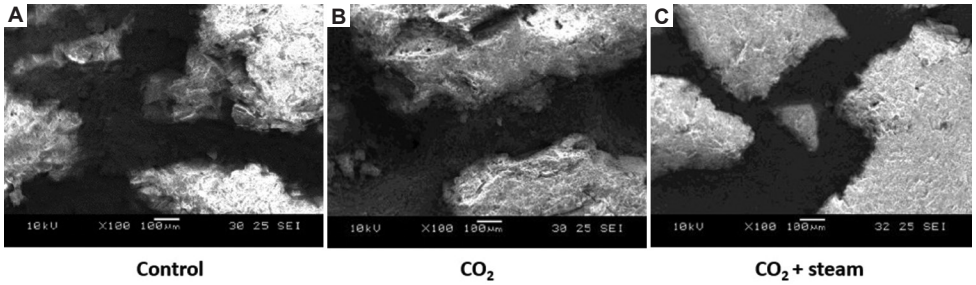

Figure 8. Scanning electron microscopy images of the microstructures of the 3D-printed large-aggregate concrete. (A) Control. (B) CO_2-treated sample. (C) Steam–CO_2-treated sample. Scale bar: 100 μm; magnification: ×100.

when the water-to-solid ratio exceeds 0.40, CO_2 uptake decreases significantly. In addition, the capability for CO_2 uptake increases with reaction time, reaching a peak between 1 and 72 h before saturation, as demonstrated in experiments with concrete slurry waste,[32] which is beyond the scope of this research.

3.4. Scanning electron microscopy of 3D-concrete-printing samples

Figure 8 displays the microstructure images of hardened concrete samples. Notably, the CO_2-treated and steam–CO_2-treated samples showed a denser and less porous region surrounding the aggregates and cement paste compared to the control sample. This indicates strong bonding between the cement paste and aggregates, contributing to the formation of a robust interfacial transition zone and enhancing the mechanical strength of the concrete samples.

3.5. CO_2 emission and cost analysis

This study conducted a computational analysis of the potential environmental impacts of 3D-printed large-aggregate concretes. The CO_2 emissions and costs associated with concrete are directly related to the quantity of materials used, particularly the cement in the mixture. The CO_2 emissions and costs associated with the strength of concrete samples were calculated under three conditions: control, CO_2, and steam–CO_2, using Equations XIV–XVII, recommended by Meng *et al.*[45]:

(i) Material cost per unit volume (USD/m^3):

$$C_M = \sum_i^i \left(m_i \times P_i\right) \quad \text{(XIV)}$$

(ii) Material cost per 1 MPa of strength (USD/MPa):

$$U_M = \frac{C_M}{f_{c(t)}} \quad \text{(XV)}$$

(iii) Carbon emission per 1 MPa of strength (kg/MPa):

$$C_{CO2} = \frac{\sum_i^i \left(m_i \times C_{CO2i}\right)}{f_{c(t)}} \quad \text{(XVI)}$$

Table 3. Materials, emission factors, and the approximate price of materials used in the study

Materials	Emission factors (kg CO_2 e/kg)	Price (USD/kg)
Cement	0.900	0.230
Stone chips	0.005	0.045
Sand	0.005	0.050
Silica fume	0.020	2.000
Superplasticizer	0.010	4.000
Water	0.0003	0.004
2 Bar CO_2	1.000	0.766
Steam	0.010	0.250
Carbon price, P_{CO2}	-	0.032

(iv) Carbon emission cost per 1 MPa of strength (USD/MPa):

$$U_{CO2} = P_{CO2} \times C_{CO2} \quad \text{(XVII)}$$

where m_i and P_i are the mass and price of each component, respectively, $f_{c(t)}$ represents the concrete strength, C_{CO2i} represents the carbon emissions from each component, and P_{CO2} represents the current average carbon price per kg of CO_2, which is USD 0.032.[46]

Table 3 presents the materials, their corresponding emission factors, and the approximate prices in the local market of Singapore. Using these equations, the approximate cost of materials, including carbon costs per 1 MPa of strength, is calculated and shown in Table 4. The results indicate that incorporating CO_2 and steam into 3D-printed concrete structures can reduce costs compared to control. Specifically, the use of a steam–CO_2 mixture resulted in a maximum cost reduction of 28% compared to control, while the use of CO_2 alone resulted in a reduction of approximately 25%. These findings suggest that combining steam with CO_2 offers greater potential than using CO_2 alone. It is important to note that other costs associated with printing, such as workforce, equipment, and transportation, were not included in this analysis, as

Table 4. Materials and carbon emissions cost per unit strength

Mix	Compressive strength (MPa)	C_M (USD/m^3)	U_M (USD/MPa)	C_{CO2} (kg/MPa)	U_{CO2} (USD/MPa)	U_M+U_{CO2} (USD/MPa)	Difference (%)
Control	21.52	390.19	18.13	29.38	0.94	19.07	0
CO_2	28.78	390.42	13.56	21.98	0.70	14.27	25.19
CO_2 + steam	29.98	390.67	13.03	21.11	0.68	13.71	28.13

Notes: C_{CO2} is the carbon emission per 1 MPa of strength; C_M is the material cost per unit volume; U_{CO2} is the carbon emission cost per 1 MPa of strength; U_M is the material cost per 1 MPa of strength.

their actual values depend on various factors that were not considered in the current calculations.

In sustainable construction, decisions should be made based on specific optimization objectives.[43] The model results presented in this research can serve as a valuable guide for these decisions. This research focused solely on the environmental impacts of the raw materials. As a result, other costs mentioned above are considered negligible. Nonetheless, the cost comparisons provided can provide readers a relative understanding of the costs of materials with or without CO_2 or a steam–CO_2 mixture during the 3D printing of structures. For a more comprehensive comparison, additional factors must be included in future calculations to develop a solid solution.

4. Conclusion

This study investigated the dual effects of CO_2 and a steam–CO_2 mixture on 3D-printed large-aggregate concrete samples. The following conclusions can be drawn from the research findings:

- The study demonstrates that employing CO_2 or steam–CO_2 in large-aggregate 3DCP has significant potential, as they can enhance both the buildability and mechanical properties of the structures.
- The buildability of 3D-printed samples is closely linked to CO_2 pressure. When CO_2 pressure increased from 2 bar to 6 bar, there was a 33% improvement in buildability for the steam–CO_2 mix compared to the control mix. However, there was no significant difference in buildability between concrete samples using CO_2 alone and those using the steam–CO_2 mixture. Notably, elevated CO_2 levels can lead to rough surface formation, detracting from achieving a smooth finish in 3D-printed structures.
- At 28 days of testing, the compressive strength of the 3D-printed samples treated with CO_2 or steam–CO2 was found to be 24% and 28% higher than that of the control samples, respectively. For flexural strength, the improvements were approximately 2% and 4%, respectively.
- The concrete samples treated with steam–CO_2 demonstrated a significant increase in CO_2 uptake compared to samples treated with only CO_2 or control. Specifically, the samples sprayed with steam–CO_2 showed 23% higher CO_2 uptake compared to the control samples.
- Regarding material and carbon costs, the integrated use of steam–CO_2 resulted in a maximum cost reduction of 28% compared to the control. For samples using CO_2 alone, the cost reduction was approximately 25%.

The primary challenge in 3D printing with large aggregates is the slump of fresh concrete. It is well established that concrete or mortar with low to zero slump is preferable for successful printing, as it prevents layer deformation. However, achieving such low-slump concrete is difficult and necessitates careful selection of material compositions and delivery systems. In addition, the lack of standardized sample sizes for various tests is concerning, as sample size can significantly affect results even when identical material compositions are used. To fully harness the benefits of this technology, these issues must be addressed through prompt collaboration between academia and industry.

Acknowledgments

None.

Funding

This research was supported by Saudi Aramco Technologies Company (SATC) and the National Research Foundation, Prime Minister's Office, Singapore, under its Medium-Sized Centre funding scheme for the Singapore Centre for 3D Printing.

Conflict of interest

The authors declare that they have no competing interests.

Author contributions

Conceptualization: Suvash Chandra Paul
Data curation: Suvash Chandra Paul
Formal analysis: Suvash Chandra Paul, Junghyun Lee, and Yi Wei Daniel Tay
Funding acquisition: Ming Jen Tan
Investigation: Suvash Chandra Paul, Junghyun Lee, Yi Wei Daniel Tay, Sean Gip Lim, Jihye Jhun, and Issam T. Amr

Methodology: Suvash Chandra Paul, Junghyun Lee, and Yi Wei Daniel Tay
Supervision: Bandar A. Fadhel, and Ming Jen Tan
Writing–original draft: Suvash Chandra Paul
Writing–review & editing: All authors

Ethics approval and consent to participate

Not applicable.

Consent for publication

Not applicable.

Availability of data

The datasets generated during and/or analyzed during the present study are available from the corresponding author on reasonable request.

Further disclosure

Parts of the findings have been presented at the Future AM 2025 conference in Singapore (August 5–7, 2025). The paper has never been uploaded to or deposited in a preprint server.

References

1. Pongwisuthiruchte A, Potiyaraj P. Challenges and innovations in sustainable 3D printing. *Mater Today Sustain*. 2025;31:101134.

   doi: 10.1016/j.mtsust.2025.101134

2. Available from: https://builtin.com/articles/3d-printed-house [Last accessed on 2025 Jun 04].

3. Jia Y, Abdelrahman S, Hauser CA. Developing a sustainable resin for 3D printing in coral restoration. *MSAM*. 2024;3(2):3125.

   doi: 10.36922/msam.3125

4. Rahul AV, Santhanam M, Meena H, Ghani Z. Mechanical characterization of 3D printable concrete. *Constr Build Mater.* 2019;227:116710.

   doi: 10.1016/j.conbuildmat.2019.116710

5. Bhattacherjee S, Basavaraj AS, Rahul AV, *et al*. Sustainable materials for 3D concrete printing. *Cem Concr Compos.* 2021;122:104156.

   doi: 10.1016/j.cemconcomp.2021.104156

6. Wolfs RJM, Bos FP, Salet TAM. Hardened properties of 3D printed concrete: The influence of process parameters on interlayer adhesion. *Cem Concr Res.* 2019;119:132-140.

   doi: 10.1016/j.cemconres.2019.02.017

7. Ding T, Xiao J, Zou S, Zhou X. Anisotropic behavior in bending of 3D printed concrete reinforced with fibers. *Compos Struct.* 2020;254:112808.

   doi: 10.1016/j.compstruct.2020.112808

8. Wang D, Xiao J, Sun B, Zhang S, Poon CS. Mechanical properties of 3D printed mortar cured by CO_2. *Cem Concr Compos.* 2023;139:105009.

   doi: 10.1016/j.cemconcomp.2023.105009

9. Haselbach L. Potential for carbon dioxide absorption in concrete. *J Environ Eng.* 2009;135(6):465-472.

   doi: 10.1061/(asce)ee.1943-7870.0000004

10. Sikora P, Techman M, Federowicz K, *et al*. Insight into the microstructural and durability characteristics of 3D printed concrete: Cast versus printed specimens. *Case Stud Constr Mat.* 2022;17:e01320.

    doi: 10.1016/j.cscm.2022.e01320

11. Sun B, Dominicus R, Dong E, Li P, Ye Z, Wang W. Predicting the strength development of 3D printed concrete considering the synergistic effect of curing temperature and humidity: From perspective of modified maturity model. *Constr Build Mater.* 2024;427:136291.

    doi: 10.1016/j.conbuildmat.2024.136291

12. Li L, Hao L, Li X, Xiao J, Zhang S, Poon CS. Development of CO_2-integrated 3D printing concrete. *Constr Build Mater.* 2023;409:134233.

    doi: 10.1016/j.conbuildmat.2023.134233

13. Kazemian M, Shafei B. Carbon sequestration and storage in concrete: A state-of-the-art review of compositions, methods, and developments. *J CO_2 Util.* 2023;70:102443.

    doi: 10.1016/j.jcou.2023.102443

14. Castellote M, Fernandez L, Andrade C, Alonso C. Chemical changes and phase analysis of OPC pastes carbonated at different CO_2 concentrations. *Mater Struct.* 2009;42:515-525.

    doi: 10.1617/s11527-008-9399-1

15. Kashef-Haghighi S, Ghoshal S. CO_2 sequestration in concrete through accelerated carbonation curing in a flow-through reactor. *Ind Eng Chem Res.* 2010;49(3):1143-1149.

    doi: 10.1021/ie900703d

16. Monkman S, Hwang SD, Khayat, K. Rheology modification of flowable mortar with CO_2. *Cem Concr Compos.* 2024;151:105584.

    doi: 10.1016/j.cemconcomp.2024.105584

17. Rahul AV, Mohan MK, De Schutter G, Van Tittelboom K. 3D printable concrete with natural and recycled coarse aggregates: Rheological, mechanical and shrinkage behaviour. *Cem Concr Compos.* 2022;125:104311.

    doi: 10.1016/j.cemconcomp.2021.104311

18. An D, Zhang YX, Yang R. Incorporating coarse aggregates into 3D concrete printing from mixture design and process control to structural behaviours and practical applications: A review. *Virtual Phys Prototyp.* 2024;19(1):e2351154.

doi: 10.1080/17452759.2024.2351154

19. Wang X, Jia L, Jia Z, *et al*. Optimization of 3D printing concrete with coarse aggregate via proper mix design and printing process. *J Build Eng.* 2022;56:104745.

doi: 10.1016/j.jobe.2022.104745

20. Li M, Weng Y, Liu Z, Zhang D, Wong TN. Optimizing of chemical admixtures for 3D printable cementitious materials by central composite design. *MSAM.* 2022;1(3):16.

doi: 10.18063/msam.v1i3.16

21. Liu H, Liu C, Wu Y, *et al*. 3D printing concrete with recycled coarse aggregates: The influence of pore structure on interlayer adhesion. *Cem Concr Compos.* 2022;134:104742.

doi: 10.1016/j.cemconcomp.2022.104742

22. Liu H, Liu C, Wu Y, *et al*. Hardened properties of 3D printed concrete with recycled coarse aggregate. *Cem Concr Res.* 2022;159:106868.

doi: 10.1016/j.cemconres.2022.106868

23. Mai I, Brohmann L, Freund N, *et al*. Large particle 3D concrete printing-a green and viable solution. *Materials (Basel).* 2021;14(20):6125.

doi: 10.3390/ma14206125

24. Wang D, Xiao J, Duan Z. Strategies to accelerate CO_2 sequestration of cement-based materials and their application prospects. *Constr Build Mater.* 2022;314:125646.

doi: 10.1016/j.conbuildmat.2021.125646

25. Singh R, Wang L, Ostrikov K, Huang J. Designing carbon-based porous materials for carbon dioxide capture. *Adv Mater Interf.* 2024;11(4):2202290.

doi: 10.1002/admi.202202290

26. Al-Khowaiter AO, Jamal A, Amr IT, Bamagain R, Al-Hunaidy AS, Fadhel BA. *Cementitious Print Head, 3D Printing Architecture, and Cementitious Printing Methodology*. Patent No. US011236517B2; 2022.

27. Lim SG, Tay YWD, Paul SC, *et al*. Carbon capture and sequestration with *in-situ* CO_2 and steam integrated 3D concrete printing. *Carbon Capture Sci Technol.* 2024;13:100306.

doi: 10.1016/j.ccst.2024.100306

28. ASTM. *C109/C109M-20: Standard Test Method for Compressive Strength of Hydraulic Cement Mortars (Using 2-in. or [50-mm] Cube Specimens)*. West Conshohocken, PA, United States: ASTM.

29. ASTM. *C293/C293M-16. Standard Test Method for Flexural Strength of Concrete (Using Simple Beam With Center-Point Loading)*. West Conshohocken, PA, United States: ASTM.

30. Bhatty JI. Hydration versus strength in a portland cement developed from domestic mineral wastes-A comparative study. *Thermochim Acta.* 1986;106:93-103.

doi: 10.1016/0040-6031(86)85120-6

31. Takahashi H, Maruyama I. Quantification of CO_2 in cement pastes with different degrees of carbonation. *J Adv Concr Technol.* 2024;22(11):706-715.

doi: 10.3151/jact.22.706

32. Fang X, Xuan D, Poon CS. Empirical modelling of CO_2 uptake by recycled concrete aggregates under accelerated carbonation conditions. *Mater Struct.* 2017;50:1-13.

doi: 10.1617/s11527-017-1066-y

33. Bernal SA, Provis JL, Mejía de Gutiérrez R, Van Deventer JS. Accelerated carbonation testing of alkali-activated slag/metakaolin blended concretes: Effect of exposure conditions. *Mater Struct.* 2015;48:653-669.

doi: 10.1617/s11527-014-0289-4

34. Kaliyavaradhan SK, Ling TC, Mo KH. CO_2 sequestration of fresh concrete slurry waste: Optimization of CO_2 uptake and feasible use as a potential cement binder. *J CO2 Util.* 2020;42:101330.

doi: 10.1016/j.jcou.2020.101330

35. Moini R, Rodriguez F, Olek J, Youngblood JP, Zavattieri PD. Mechanical properties and fracture phenomena in 3D-printed helical cementitious architected materials under compression. *Mater Struct.* 2024;57(7):170.

doi: 10.1617/s11527-024-02437-4

36. Panda B, Paul SC, Tan MJ. Anisotropic mechanical performance of 3D printed fiber reinforced sustainable construction material. *Mater Lett.* 2017;209:146-149.

doi: 10.1016/j.matlet.2017.07.123

37. Pi Y, Lu C, Li B, Zhou J. Crack propagation and failure mechanism of 3D printing engineered cementitious composites (3DP-ECC) under bending loads. *Constr Build Mater.* 2023;408:133809.

doi: 10.1016/j.conbuildmat.2023.133809

38. Wang YC, Lee MG, Wang WC, Kan YC, Kao SH, Chang HW. CO_2 curing on the mechanical properties of Portland cement concrete. *Buildings.* 2022;12(6):817.

doi: 10.3390/buildings12060817

39. Shi C, Wu Y. Studies on some factors affecting CO_2 curing of lightweight concrete products. *Resour Conserv Recycle.* 2008;52(8-9):1087-1092.

doi: 10.1016/j.resconrec.2008.05.002

40. Kamal NLM, Itam Z, Sivaganese Y, Beddu S. Carbon dioxide sequestration in concrete and its effects on concrete compressive strength. *Mater Today Proc.* 2020;31:A18-A21.

doi: 10.1016/j.matpr.2020.11.185

41. Lippiatt N, Ling TC. Rapid hydration mechanism of carbonic acid and cement. *J Build Eng.* 2020;31:101357.

doi: 10.1016/j.jobe.2020.101357

42. Han Y, Meng LY, Lin R, Kim S, Kim T, Wang XY. Evaluating the sustainability of microwave pre-cured high-volume slag concrete: Mechanical properties, environmental impact and cost-benefit analysis. *J Build Eng.* 2024;96:110663.

    doi: 10.1016/j.jobe.2024.110663

43. Gao Y, Jiang Y, Tao Y, Shen P, Poon CS. Accelerated carbonation of recycled concrete aggregate in semi-wet environments: A promising technique for CO_2 utilization. *Cem Concr Res.* 2024;180:107486.

    doi: 10.1016/j.cemconres.2024.107486

44. Dixit A, Du H, Dai Pang S. Carbon capture in ultra-high performance concrete using pressurized CO_2 curing. *Constr Build Mater.* 2021;288:123076.

    doi: 10.1016/j.conbuildmat.2021.123076

45. Meng LY, Wang YS, Sun F, Lin R, Wang XY. An integrated strength-carbon emissions-total cost model for silica fume concrete. *Case Stud Constr Mat.* 2025;22:e04327.

    doi: 10.1016/j.cscm.2025.e04327

46. O˘Guz S, Bellefontaine R, West J. Visualized: The Price of Carbon around the World in 2024. Available from: https://www.visualcapitalist.com/sp/visualized-the-price- of-carbon-around-the-world-in-2024 [Last accessed on 2025 Jul 24].